3. Photon number fluctuations

In the circuit QED architecture, resonator *photon number fluctuation* is another major decoherence source[147]. Residual microwave fields in the cavity have photon-number fluctuations that in the dispersive regime impact the qubit through an interaction term $\chi\sigma_z n$, see Sec. II C 2, leading to a frequency shift $\Delta_{\rm Stark} = 2\eta\chi\bar{n}$, where $\bar{n}$ is the average photon number, and $\eta = \kappa^2/(\kappa^2 + 4\chi^2)$ effectively scales the photon population seen by the qubit due to the interplay between the qubit-induced dispersive shift of the resonator frequency (χ) and the resonator decay rate (κ).

In the dispersive limit, the noise is longitudinally coupled to the qubit and leads to pure dephasing at a rate,

$$\Gamma_\phi = \eta\frac{4\chi^2}{\kappa}\bar{n}. \tag{51}$$

The fluctuations originate from residual photons in the resonator, typically due to radiation from higher temperature stages in the dilution refrigerator[107,148]. The corresponding noise spectral density is of a Lorentzian type,

$$S(\omega) = 4\chi^2\frac{2\eta\bar{n}\kappa}{\omega^2+\kappa^2}, \tag{52}$$

which exhibits an essentially white noise spectrum up to a 3dB cutoff frequency $\omega = \kappa$ set by the resonator decay rate κ, see Ref. 62.

4. Quasiparticles

Quasiparticles, i.e. unpaired electrons, are another important noise source for superconducting devices[121]. The tunneling of quasiparticles through a qubit junction may lead to both T_1 relaxation and pure dephasing T_φ, depending on the type of qubit, the bias point, and the junction through which the tunneling event occurs[120,122].

Quasiparticles are naturally excited due to thermodynamics, and the quasiparticle density in equilibrium superconductors should be exponentially suppressed as temperature decreases. However, below about 150 mK, the quasiparticle density observed in superconducting devices – generally in the range $10^{-8}-10^{-6}$ per Cooper pair – is much higher than BCS theory would predict for a superconductor in equilibrium with its cryogenic environment at 10 mK. The reason for this excess quasiparticle population is unclear, but it is very likely related to the presence of additional, non-thermal mechanisms that increase the generation rates, "bottleneck effects" that occur at millikelvin temperatures to reduce recombination rates, or a combination of both.

It has been shown that the observed T_1 and excess excited-state population measured in today's state-of-the-art high-coherence transmon are self-consistent with excess "hot" nonequilibrium quasiparticles at the quasi-universal density of around $10^{-7} - 10^{-6}$ per Cooper pair[149,150]. Although this quasiparticle generation mechanism is not yet well understood, it has been shown that quasiparticles can be transiently pumped away, improving T_1 times and reducing T_1 temporal variation[122].

D. Operator form of qubit-environment interaction

Similar to the way that two qubits are coupled, a qubit may couple and interact with uncontrolled degrees of freedom (DOF) in its environment (the noise sources). The interaction Hamiltonian between the qubit DOF ($\hat{O}_q$) and those of the noise source ($\hat{\lambda}$) may be expressed in a general form

$$\hat{H}_{\rm int} = \nu\hat{O}_q\hat{\lambda} \tag{53}$$

where ν denotes the coupling strength – which is related to the sensitivity of the qubit to environmental fluctuations $\partial\hat{H}_q/\partial\lambda$ – and we assume that $\hat{O}_q$ is a qubit operator within the qubit Hamiltonian $\hat{H}_q$. The noisy environment represented by the operator $\hat{\lambda}$ produces fluctuations $\delta\lambda$. Note that we retained the hats in this section to remind us that these are quantum operators.

1. Connecting T_1 to $S(\omega)$

If the coupling is transverse to the qubit, e.g. $\hat{O}_q$ is of the type σ_x or $(a + a^\dagger)$ – see the related case of qubit-qubit coupling treated in Sec. II C – then noise at the qubit frequency can cause transitions between the qubit eigenstates. Since this is a stochastic process, the ensemble-average manifests itself as a decay (usually exponential) of the qubit population towards a certain equilibrium value (usually the qubit ground state $|0\rangle$ for $k_BT \ll \hbar\omega_{\rm q}$). Again, this process is equivalently referred to as "T_1 relaxation", "energy relaxation", or "longitudinal relaxation". As stated above, T_1 is the characteristic time scale of the decay. Its inverse, $\Gamma_1 = 1/T_1$ is called the relaxation rate and depends on the power spectral density of the noise $S(\omega)$ at the transition frequency of the qubit $\omega = \omega_{\rm q}$:

$$\Gamma_1 = \frac{1}{\hbar^2}\left|\langle 0|\frac{\partial\hat{H}_q}{\partial\lambda}|1\rangle\right|^2 S_\lambda(\omega_{\rm q}), \tag{54}$$

where $\partial\hat{H}_q/\partial\lambda$ is the qubit transverse susceptibility to fluctuations $\delta\lambda$, such that $|\delta\lambda|^2$ is the ensemble average value of the environmental noise sources as seen by the qubit. Eq. (54) is equivalent to Fermi's Golden Rule, in which the qubit's transverse susceptibility to noise is driven by the noise power spectral density. The qubit transverse susceptibility can be used to calculate the prefactors; for example, for fluctuations $\delta\lambda = \delta n$, the relevant term in the transmon Hamiltonian in Eq. (16) is

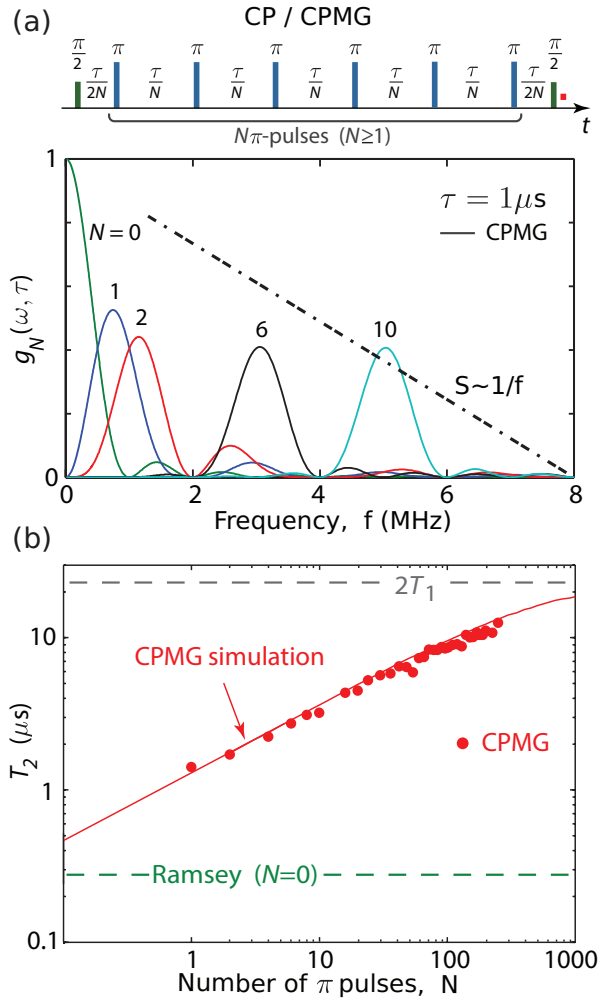

FIG. 7. Dynamical error suppression. **(a)** Carr-Purcell-Meiboom-Gill (CPMG) pulse sequence applies N equally spaced π pulses within an otherwise free-evolution time τ. Pulses in the time domain correspond to bandpass filters in the frequency domain (lower panel) which serve to shape the noise power spectrum seen by the qubit. The centroid of the bandpass filter shifts to higher frequencies as N is increased. For noise that decreases with frequency, such as $1/f$ noise, larger N corresponds to less integrated noise impinging on the qubit. **(b)** CPMG pulse sequence applied to a flux qubit biased at a point that is highly sensitive to $1/f$ flux noise. The Ramsey ($N = 0$) time is approximately 300 ns, and the Hahn echo ($N = 1$) time is approximately 1.5 μs. Increasing the number of CPMG pulses continues to increase the effective T_2 time towards the $2T_1$ limit. Adapted from Ref. 78.

$4E_C(\hat{n} - n_g)^2$, where we allow for an offset charge n_g, and the susceptibility is given by $8E_C\hat{n}$. We refer the reader to Refs. 151–153 for more details.

2. *Connecting T_φ to $S(\omega)$*

If the coupling to the qubit is instead longitudinal, e.g. $\hat{H}_q$ is of the type σ_z or $a^\dagger a$, the noise will stochastically modulate the transition frequency of the qubit and thereby introduce a stochastic phase evolution of a qubit superposition state. This gradually leads to a loss of phase information, and it is therefore called *pure dephasing* (time constant T_φ). Unlike T_1 relaxation, which is generally an irreversible (incoherent) error, pure dephasing T_φ is in principle reversible (a coherent error). The degree of pure dephasing depends on the control pulse sequence applied while the qubit is subject to the noise process.

Consider the relative phase φ of a superposition state undergoing free evolution in the presence of noise. The superposition state's accumulated phase,

$$\varphi(t) = \int_0^t \omega_q dt' = \langle\omega_{\rm q}\rangle t + \delta\varphi(t) \tag{55}$$

diffuses due to adiabatic fluctuations of the transition frequency,

$$\delta\varphi(t) = \frac{\partial\omega_{\rm q}}{\partial\lambda}\int_0^t \delta\lambda(t')\mathrm{d}t', \tag{56}$$

where $\partial\omega_{\rm q}/\partial\lambda = (1/\hbar)|\langle\partial\hat{H}_q/\partial\lambda\rangle|$ is the qubit's longitudinal sensitivity to λ-noise. For noise generated by a large number of fluctuators that are weakly coupled to the qubit, its statistics are Gaussian. Ensemble averaging over all realizations of the Gaussian-distributed stochastic process $\delta\lambda(t)$, the dephasing is

$$\langle e^{i\,\delta\varphi(t)}\rangle = e^{-\frac{1}{2}\langle\delta\varphi^2(t)\rangle} \equiv e^{-\chi_N(t)}, \tag{57}$$

leading to a coherence decay function,

$$\langle e^{-\chi_N(\tau)}\rangle = \exp\left[-\frac{\tau^2}{2}\frac{\partial\omega_{\rm q}}{\partial\lambda}\int_{-\infty}^{\infty} g_N(\omega,\tau)S(\omega)d\omega\right], \tag{58}$$

where $g(\omega,\tau)$ is a dimensionless weighting function.

The function $g_N(\omega,\tau)$ can be viewed as a frequency-domain filter of the noise $S_\lambda(\omega)$ [see Fig. 7(a)]. In general, its filter properties depend on the number N and distribution of applied pulses. For example, considering sequences of π-pulses[78,154–158],

$$g_N(\omega,\tau) = \frac{1}{(\omega\tau)^2}\Big|1 + (-1)^{1+N}\exp(i\omega\tau) + 2\sum_{j=1}^{N}(-1)^j\exp(i\omega\delta_j\tau)\cos(\omega\tau_\pi/2)\Big|^2, \tag{59}$$

where $\delta_j \in [0,1]$ is the normalized position of the centre of the jth π-pulse between the two $\pi/2$-pulses, τ is the total free-induction time, and τ_π is the length of each π-pulse[157,158], yielding a total sequence length $\tau + N\tau_\pi$. As the number of pulses increases for fixed τ, the filter function's peak shifts to higher frequencies, leading to a reduction in the net integrated noise for $1/f^\alpha$-type noise spectra with $\alpha > 0$. Similarly, for a fixed N, the filter

function will shift in frequency with τ. Additionally, for a fixed time separation $\tau' = \tau/N$ (valid for $N \geq 1$), the filter sharpens and asymptotically peaks at $\omega'/2\pi = 1/2\tau'$ as more pulses are added. $g_N(\omega, \tau)$ is thus called the "filter function"[78,156], and it depends on the pulse sequences being applied. From Eq. (58), the pure dephasing decay arises from a noise spectral density that is "shaped" or "filtered" by the sequence-specific filter function. By choosing the number of pulses, their rotation axes, and their arrangement in time, we can design filter functions that minimize the net noise power for a given noise spectral density within the experimental constraints of the experiment (e.g., pulse-modulation bandwidth of the electronics used to control the qubits).

To give a standard example, we compare the coherence integral for two cases: a Ramsey pulse sequence and a Hahn echo pulse sequence. Both sequences involve two $\pi/2$ pulses separated by a time τ, during which free evolution of the qubit occurs in the presence of low-frequency dephasing noise. The distinction is that the Hahn echo will place a single π pulse ($N = 1$) in the middle of the free-evolution period, whereas the Ramsey does not use any additional pulses ($N = 0$). The resulting filter functions are:

$$g_0(\omega, \tau) = \text{sinc}^2 \frac{\omega\tau}{2} \tag{60}$$

$$g_1(\omega, \tau) = \sin^2 \frac{\omega\tau}{4} \text{sinc}^2 \frac{\omega\tau}{4} \tag{61}$$

where the subscript $N = 0$ and $N = 1$ indicate the number of π-pulses applied for the Ramsey and Hahn echo experiments, respectively. The filter function $g_0(\omega, \tau)$ for the Ramsey case is a sinc-function centered at $\omega = 0$. For noise that decreases with frequency, e.g., $1/f$ flux noise in superconducting qubits, the Ramsey experiment windows through the noise in $S(\omega)$ where it has its highest value. This is the worst choice of filter function for $1/f$ noise. In contrast, the Hahn echo filter function has a centroid that is peaked at a higher frequency, away from $\omega = 0$. In fact, it has zero value at $\omega = 0$. For noise that decreases with frequency, such as $1/f$ noise, this is advantageous. This concept extends to larger numbers N of π pulses, and is called a Carr-Purcell-Meiboom-Gill (CPMG) sequence[159,160]. In Fig. 7(b), the T_2 time of a qubit under the influence of strong dephasing noise is increased toward the $2T_1$ limit using a CPMG dynamical error-suppression pulse sequence with an increasing number of pulses, N. We refer the reader to Refs. 78, 161, and 162, where these experiments were performed with superconducting qubits.

3. Noise spectroscopy

The qubit is highly sensitive to its noisy environment, and this feature can be used to map out the noise power spectral density. In general, one can map the noise PSD during *free evolution* – periods of time for which no control is applied to the qubit, except for very short dynamical decoupling pulses – and during *driven evolution* – periods of time during which the control fields are applied to the qubit. Both free-evolution and driven-evolution noise is important to characterize, as the noise PSD may differ for these two types of evolution, and both are utilized in the context of universal quantum computation. We refer the reader to Ref. 132 for a summary of noise spectroscopy during both types of evolution.

The Ramsey frequency itself is sensitive to longitudinal noise, and monitoring its fluctuations is one means to map out the noise spectral density over the sub-millihertz to ~ 100 Hz range[131,163].

At higher frequencies, the CPMG dynamical decoupling sequence can be used to create narrow-band filters that "sample" the noise at different frequencies as a function of the free-evolution time τ and the number of pulses N. This has been used to map out the noise PSD in the range 0.1 - 300 MHz[78]. One must be careful of the additional small peaks at higher-frequencies, which all contribute to the dephasing used to perform the noise spectroscopy[164].

In fact, using pulse envelopes such as Slepians[165] – which are designed to have concentrated frequency response – to perform noise spectroscopy is one means to reduce such errors[157].

At even higher frequencies, measurements of T_1 can be used in conjunction with Fermi's golden rule to map out the transverse noise spectrum above 1 GHz[62,78,166].

The aforementioned are all examples of noise spectroscopy during free evolution. Noise spectroscopy during driven evolution was also demonstrated using a "spin-locking" technique, where a strong drive along x or y axes defines a new qubit quantization axis, whose Rabi frequency is the new qubit frequency in the spin-locking frame. The spin-locking frame is then used to infer the noise spectrum while the qubit is continually subject to a driving field. For more information, we refer the reader to Ref. 132.

E. Engineering noise mitigation

Here, we briefly review a few examples of techniques that have been developed to reduce noise or reduce its impact on decoherence (sensitivity). We stress that improving gate fidelity is a comprehensive optimization task, one that is full of trade-offs. It is thus important to identify what the limiting factors are, what price we have to pay to diminish these limiting factors, and what advantage we can achieve until reaching a better trade-off. These all require an accurate understanding the limitations on the gate fidelity, the sources of decoherence, the properties of the noise, and how it affects the system performance.